Arf3p GTPase is a key regulator of Bud2p activation for invasive growth in *Saccharomyces cerevisiae*

Jia-Wei Hsu and Fang-Jen S. Lee
Institute of Molecular Medicine, College of Medicine, National Taiwan University, and Department of Medical Research, National Taiwan University Hospital, Taipei 100, Taiwan

ABSTRACT **The regulation and signaling pathways involved in the invasive growth of yeast have been studied extensively because of their general applicability to fungal pathogenesis. Bud2p, which functions as a GTPase-activating protein (GAP) for Bud1p/Rsr1p, is required for appropriate budding patterns and filamentous growth. The regulatory mechanisms leading to Bud2p activation, however, are poorly understood. In this study, we report that ADP-ribosylation factor 3p (Arf3p) acts as a regulator of Bud2p activation during invasive growth. Arf3p binds directly to the N-terminal region of Bud2p and promotes its GAP activity both in vitro and in vivo. Genetic analysis shows that deletion of *BUD1* suppresses the defect of invasive growth in *arf3*Δ or *bud2*Δ cells. Lack of Arf3p, like that of Bud2p, causes the intracellular accumulation of Bud1p-GTP. The Arf3p–Bud2p interaction is important for invasive growth and facilitates the Bud2p–Bud1p association in vivo. Finally, we show that under glucose depletion–induced invasion conditions in yeast, more Arf3p is activated to the GTP-bound state, and the activation is independent of Arf3p guanine nucleotide-exchange factor Yel1p. Thus we demonstrate that a novel spatial activation of Arf3p plays a role in regulating Bud2p activation during glucose depletion–induced invasive growth.**

Monitoring Editor
Fred Chang
Columbia University

Received: Mar 11, 2013
Revised: May 16, 2013
Accepted: Jun 7, 2013

INTRODUCTION

Cell polarization is crucial for cell proliferation, differentiation, and morphogenesis in both unicellular and multicellular organisms. The determinants of polarity can be either internally or externally derived (Howell and Lew, 2012). In general, polarity establishment can be described in terms of the following steps: stimulation of spatial cues, determination of landmark proteins, subsequent recruitment of signaling molecules, and asymmetric organization of the cytoskeleton. Of note, small GTPase modules function as key signaling molecules in polarity establishment (Irazoqui and Lew, 2004; Park and Bi, 2007). The yeast *Saccharomyces cerevisiae* has been used as a model organism for studying the development of polarity, showing three unique life cycle stages of polarized growth—budding, mating, and filamentous growth—among which the mechanisms underlying budding have been the best studied (Park and Bi, 2007). Yeast reproduces via asymmetric division, giving rise to a daughter cell, during which the selection process for determining the budding site is highly organized and exhibits a unique pattern (Park and Bi, 2007; Perez and Rincon, 2010). The machinery required to specify the axial budding pattern of haploid yeast has been identified as a GTPase module composed of Bud1p (Rsr1p), Bud2p, and Bud5p (Bender, 1993). The GTPase Bud1p is activated by its guanine nucleotide exchange factor (GEF), Bud5p, and activated Bud1p subsequently recruits Cdc24p, the GEF for Cdc42p, to the presumptive bud site (Bender, 1993). The GTPase-activating protein (GAP) Bud2p then promotes the hydrolysis of Bud1p-GTP to trigger the activation of Cdc24p, which in turn activates Cdc42p to regulate the actin reorganization required for polarized growth (Leberer *et al.*, 1996). Therefore Bud1p GTP–GDP cycling is believed to be necessary for bud-site selection and to link spatial landmarks to polarity establishment (Kang *et al.*, 2010; Perez and Rincon, 2010).

ADP-ribosylation factors (Arfs) are highly conserved small GTPases that are major regulators of vesicular trafficking and cytoskeletal reorganization (Chavrier and Menetrey, 2010; Donaldson and Jackson, 2011). Yeast Arf3p is the homologue of mammalian Arf6, which is involved in multiple cellular processes, including cell adhesion,

This article was published online ahead of print in MBoC in Press (http://www.molbiolcell.org/cgi/doi/10.1091/mbc.E13-03-0136) on June 19, 2013.

Address correspondence to: Fang-Jen S. Lee (fangjen@ntu.edu.tw).

Abbreviations used: Arf, ADP-ribosylation factor; GAP, GTPase-activating protein; GEF, guanine nucleotide exchange factor.

migration, wound healing, membrane ruffling, and metastasis (D'Souza-Schorey and Chavrier, 2006). Although Arf3p and Arf6 are 75% similar in their amino acid sequences, the functions of these two proteins are distinct. Arf3p is involved in actin organization and polarity development during yeast budding (Huang *et al.*, 2003; Zakrzewska *et al.*, 2003; Costa and Ayscough, 2005; Lambert *et al.*, 2007), although the detailed molecular mechanisms underlying the function of Arf3p during polarity development have not been elucidated.

Several fungi, including *S. cerevisiae*, can undergo a developmental switch from vegetative growth to filamentous growth to survive in a stressed environment (Park and Bi, 2007). There are two forms of filamentous growth in *S. cerevisiae*, invasive growth and pseudohyphal growth, depending on ploidy and growth conditions (Pan *et al.*, 2000; Cullen and Sprague, 2012). The regulatory network associated with haploid yeast invasive growth and the cooperative signaling that occurs during this process have been extensively studied, and many key molecules involved in polarity development during yeast vegetative growth have been found to also be required for invasive growth (Pan *et al.*, 2000; Cullen and Sprague, 2002; Palecek *et al.*, 2002). For example, Bud2p, the critical regulator of bud site selection during yeast budding, has been shown to be required for yeast invasive growth (Jin *et al.*, 2008) and invasive hyphal morphogenesis in *Candida albicans* (Hausauer *et al.*, 2005).

Given these observations, we hypothesized that Arf3p may also participate in the yeast invasive growth and found that the Arf3p–Bud2p interaction is important for invasive growth by regulating Bud2p GAP activity toward Bud1p. Furthermore, we found that the activity of Arf3p is stimulated upon glucose depletion. Together the results of our study identify Arf3p as an upstream regulator of Bud2p and suggest the existence of a novel small GTPase cascade, Arf3p-Bud2p-Bud1p, which orchestrates polarity development during invasive growth.

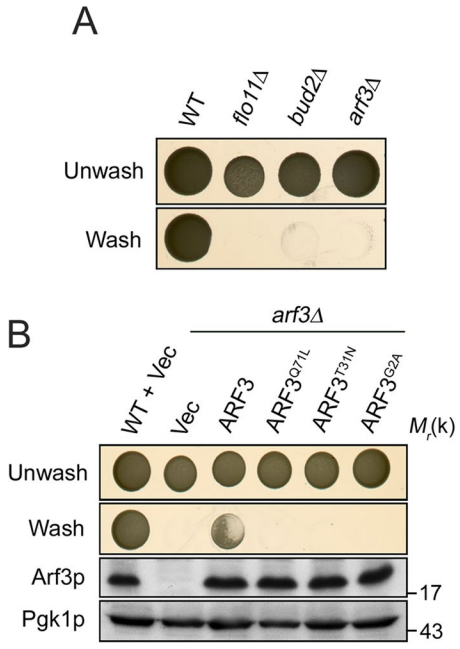

FIGURE 1: Arf3p is required for yeast invasive growth. (A) Both Arf3p and Bud2p are required for yeast invasive growth. Equal concentrations of wild-type, *flo11*Δ, *bud2*Δ, and *arf3*Δ cells with yeast Σ1278b were spotted onto YPD plates and incubated for 3 d at 30°C. The plates were photographed before (top) and after (bottom) rinsing with water. (B) Expression of wild-type Arf3p rescues yeast invasive growth in *arf3*Δ mutant cells. Wild-type or *arf3*Δ yeast Σ1278b cells transformed with an empty vector and *arf3*Δ mutant cells transformed with the indicated plasmids were spotted onto YPD plates to examine agar penetration after washing. Protein extracts from the indicated strains were resolved by SDS–PAGE, and the indicated proteins were detected by immunoblot with anti-Arf3p and anti-Pgk1p (internal control) antibodies.

RESULTS

Arf3p is required for yeast invasive growth

Many proteins that are involved in polarized growth in yeast also participate in invasive growth (Cullen and Sprague, 2002). Furthermore, a previous large-scale screening analysis suggested that Bud2p is involved in the maintenance of yeast invasive growth (Park *et al.*, 1993; Cullen and Sprague, 2002; Jin *et al.*, 2008). Because both Arf3p and Bud2p participate in the regulation of polarity process, we speculate that Arf3p might also participate in yeast invasive growth. Therefore we examined the invasive growth of *ARF3* and *BUD2* deletion mutants using the haploid yeast strain Σ1278b, which is commonly used to study invasive growth and agar penetration (Gimeno *et al.*, 1992). We found that both the *arf3*Δ and *bud2*Δ mutations impaired agar invasion, which is a classic phenomenon of yeast invasive growth (Figure 1A). The cell surface flocculin Flo11p is required for yeast invasion (Lo and Dranginis, 1998) and thus was used as a control for agar invasion defects (Figure 1A). This phenotype of *arf3*Δ cells could be significantly restored via the expression of wild-type Arf3p. The constitutively active form ($Arf3p^{Q71L}$), the GTP-binding–defective mutant ($Arf3p^{T31N}$), and the membrane-binding–defective mutant ($Arf3p^{G2A}$), however, were all unable to restore the phenotype (Figure 1B). These data suggest that dynamic cycling of GTP- and GDP-bound Arf3p at the plasma membrane is required for yeast invasive growth.

Arf3p directly interacts with Bud2p in a GTP-dependent manner

A potential physical interaction between Bud2p and Arf3p was indicated from a large-scale yeast two-hybrid analysis (Hazbun *et al.*, 2003). To explore the underlying mechanism of Arf3p functioning in yeast invasion, we first verified this interaction with yeast two-hybrid analyses. We observed that Arf3p interacts with full-length Bud2p, and the constitutively active mutant $Arf3p^{Q71L}$, which cannot hydrolyze GTP, strongly interacts with Bud2p (Figure 2A). On the other hand, the constitutively inactive $Arf3p^{T31N}$ mutant, which cannot bind GTP, cannot interact with Bud2p (Figure 2A). The interaction is Arf3p specific because no interaction was detected between Bud2p and other constitutively active Arf or Arf-like (Arl) proteins (Figure 2B). To examine the Arf3p–Bud2p interaction in vivo, we coexpressed Arf3p (wild type, Q71L, or T31N) and hemagglutinin (HA)-tagged Bud2p in *arf3*Δ cells. HA-Bud2p was immunoprecipitated, and we detected bound Arf3p and $Arf3p^{Q71L}$ but not $Arf3p^{T31N}$ (Figure 2C).

Bud2p contains two functional domains: a C2 domain for membrane targeting and a GAP domain to facilitate Bud1p-GTP hydrolysis. To map the Arf3p-interacting region of Bud2p, we expressed and purified various glutathione *S*-transferase (GST)–tagged fragments of Bud2p (Bud2N, Bud2C2, Bud2GAP, and Bud2CT), as illustrated in Figure 2D, and examined their interaction with histidine (His)-tagged $Arf3^{Q71L}$ or $Arf3^{T31N}$ using in vitro pull-down assays. We found that Bud2N (N-terminal 336 amino acids) was able to interact with $Arf3^{Q71L}$ (Figure 2E). Further truncation of the N-terminus of Bud2p indicated that the first 120 residues (Bud2N1) are sufficient for the interaction with $Arf3^{Q71L}$ (Figure 2F). This interaction was further examined by using purified His-Arf3 prebound with GTPγS or GDP and GST-Bud2N1. We also found that Bud2N1 specifically interacts with Arf3-GTPγS but not Arf3-GDP (Supplemental Figure S1).

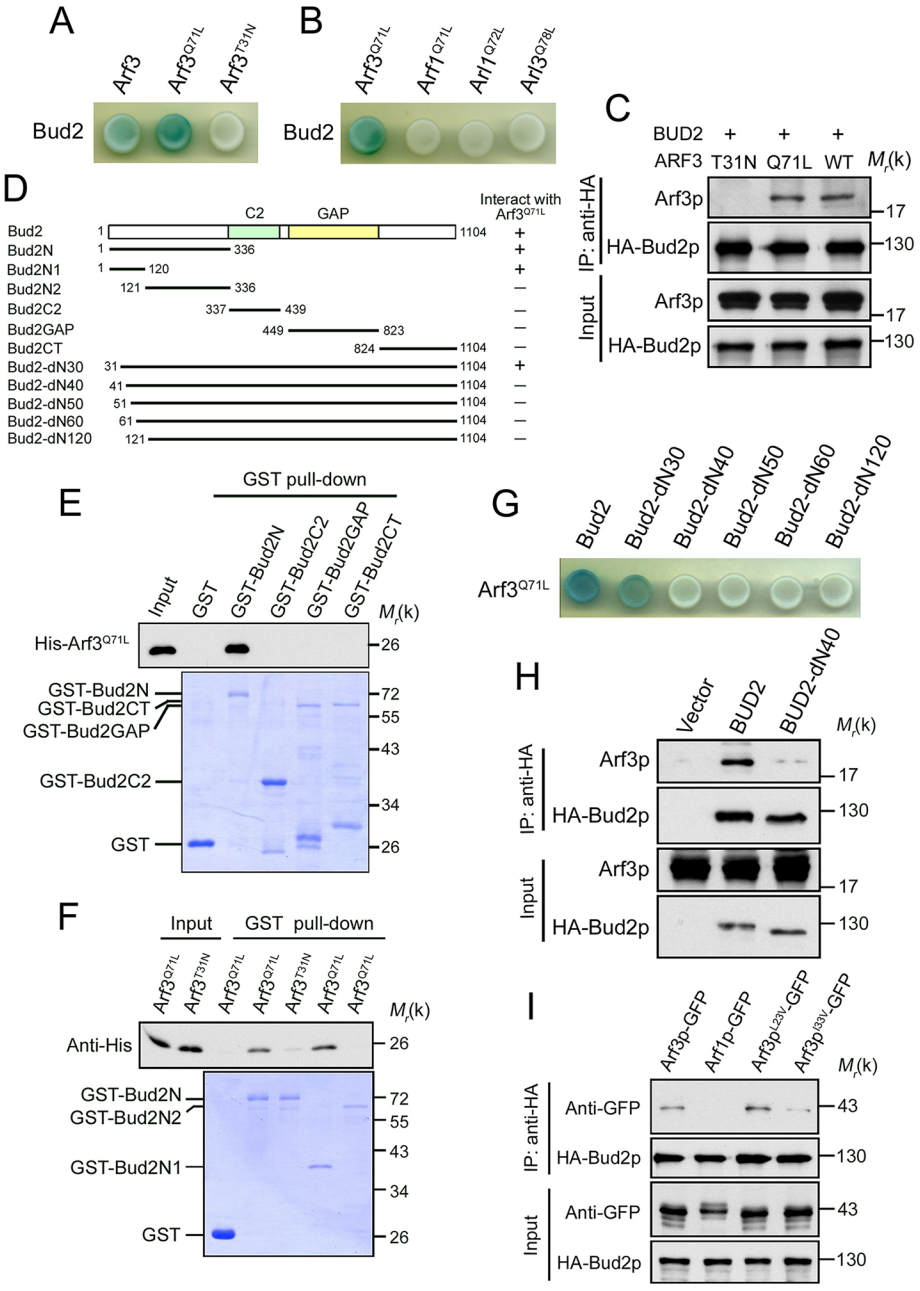

FIGURE 2: Arf3p specifically and directly interacts with Bud2p. (A) Bud2p interacts with Arf3p in a GTP-dependent manner. Bait plasmids (pEG202) containing various *ARF3* constructs (wild type, Q71L, or T31N) were cotransformed with the pJG4-5 plasmid containing *BUD2* into yeast YEM1α, and their interactions were analyzed in a β-galactosidase assay. (B) Bud2p specifically interacts with active forms of Arf3p. *BUD2*/pJG4-5 was cotransformed with different active Arf family members, and their interaction was indicated by the development of a blue color. (C) Arf3p associates with Bud2p in vivo. Each of the indicated Arf3p variants was expressed in yeast Σ1278b cells with HA-Bud2p. As described in *Materials and Methods*, HA-Bud2p was immunoprecipitated with an anti-HA antibody, and the bound proteins were assayed for the presence of different forms of Arf3p. (D) Schematic representation of the various constructs containing the *BUD2* truncation mutants. (E) Arf3p interacts with the N-terminus of Bud2p in vitro. Purified His-Arf3^{Q71L} was incubated with recombinant GST, GST-Bud2-N, GST-Bud2C2, GST-Bud2GAP, or GST-Bud2CT for 1 h. The proteins were pulled down with glutathione–Sepharose 4B beads and visualized via immunoblotting with an anti-His antibody. (F) The N-terminal 120 amino acids of Bud2p interact with Arf3p in vitro. Purified His-Arf3^{Q71L} was incubated with recombinant GST, GST-Bud2-N, GST-Bud2N1, or GSTT-Bud2N2 for 1 h. The proteins were pulled down with glutathione–Sepharose 4B beads and visualized via immunoblotting with an anti-His antibody. (G) Bud2p interacts with Arf3p^{Q71L} via the N-terminal region. Interactions of N-terminal truncations of Bud2p depicted in D with the active form of Arf3p were examined using a yeast two-hybrid assay. (H) Bud2p-dN40 dissociates from Arf3p in vivo. Σ1278b yeast cells overexpressing Arf3p were cotransformed with the indicated expression vectors. HA-Bud2p or HA-Bud2p-dN40 was immunoprecipitated with an anti-HA antibody, and the bound proteins were assayed for the presence of Arf3p. (I) Isoleucine 33 of Arf3p is essential for the interaction of Arf3p with Bud2p. The indicated Arf proteins were expressed in Σ1278b yeast cells with HA-Bud2p. HA-Bud2p was immunoprecipitated with an anti-HA antibody, and the bound proteins were assayed by immunoblotting.

Moreover, a series of N-terminal truncations of Bud2p was examined for potential interaction with Arf3p via yeast two-hybrid analysis, revealing that the N-terminal 40 residues of Bud2p are necessary for interaction with Arf3p (Figure 2G). The requirement for the N-terminal 40 amino acids of Bud2p for interaction with Arf3p was also observed in vivo (Figure 2H). These data demonstrate that Arf3p interacts directly with the N-terminal region of Bud2p in a GTP-dependent manner.

To identify the critical amino acids in Arf3p responsible for the interaction with Bud2p, we first generated two Arf1p–Arf3p chimeras: ARF3N1C, which contains amino acids 1–77 of Arf3p and amino acids 78–181 of Arf1p, and ARF1N3C, which contains amino acids 1–77 of Arf1p and amino acids 78–183 of Arf3p (Supplemental Figure S2A). A coimmunoprecipitation experiment using cells expressing chimeric Arf proteins and HA-Bud2p demonstrated that the N-terminus of Arf3p is the major region involved in the interaction with Bud2p (Supplemental Figure S2A). To further identify the specific residues within the N-terminus of Arf3p that is important for this interaction, we aligned the N-terminal sequences of yeast Arf1p and Arf3p with the Arf3p human homologue, Arf6 (Supplemental Figure S2B). We identified two residues, L23 and I33, in Arf3p that are conserved in yeast Arf3p and human Arf6 but not yeast Arf1p. Hence, we mutated these two residues in Arf3p to valine, which is the corresponding amino acid in Arf1p, and analyzed the localization and interaction abilities of the mutant proteins. We observed that although Arf3p^{L23V}–green fluorescent protein (GFP) and Arf3p^{I33V}-GFP exhibited similar subcellular distributions compared with wild-type Arf3p based on microscopic observations and fractionation analysis (Supplemental Figure S2, C and D), coimmunoprecipitation analysis revealed that the interaction

between Arf3p^{I33V} and HA-Bud2p was weakened (Figure 2I). Of interest, neither L23 nor I33 of Arf3p was required for interaction with its GEF, Yel1p (Gillingham and Munro, 2007), or its polarization partner, Afi1p (Tsai *et al.*, 2008), in yeast two-hybrid analysis (Supplemental Figure S2E). These data indicate that I33 of Arf3p specifically contributes to the Arf3p–Bud2p interaction. Collectively our data demonstrate that I33 of Arf3p and the N-terminal 40 residues of Bud2p are the regions responsible for the Arf3p–Bud2p interaction.

Arf3p and Bud2p partially colocalize at the emerging bud

Arf3p localizes to the plasma membrane and is enriched at the emerging bud (Huang *et al.*, 2003); Bud2p, however, localizes to the presumptive bud site and subsequently to the mother–bud neck after bud emergence (Park *et al.*, 1999). Therefore it is not surprising that we observed colocalization of Arf3p-mRFP and GFP-Bud2p at the mother–bud neck (Supplemental Figure S3A). Nevertheless, upon careful observation we noticed a subtle difference in the distributions of these two proteins: Arf3p–monomeric red fluorescent protein (mRFP) was enriched at both the plasma membrane of the daughter cell and the neck, whereas GFP-Bud2p was mainly concentrated at the mother–bud neck (Supplemental Figure S3). These data indicate that Bud2p and Arf3p only partially colocalize during polarized growth. Indeed, we found that the membrane targeting and polarized distribution of Arf3p and Bud2p are independent of each other, as GFP-Bud2p localized to the bud neck in both wild-type and *arf3*Δ cells (Supplemental Figure S3B), and Arf3p-GFP displayed a highly polarized membrane distribution in both wild-type and *bud2*Δ cells (Supplemental Figure S3C). These data indicate that the polarized distribution of Arf3p and Bud2p is independent of their physical interaction.

The Arf3p–Bud2p interaction is important for yeast invasive growth

Given that Arf3p interacts with Bud2p and they share similar phenotypes in yeast invasive growth, we next examined whether the Arf3p–Bud2p interaction is required for yeast invasive growth. We found that agar invasion was restored in *bud2*Δ cells via the expression of wild-type Bud2p and Bud2p-dN30 but not through the expression of the Arf3p-binding defective mutant Bud2p-dN40 (Figure 3A). Deletion of the N-terminal 40 amino acids of Bud2p may not affect the global conformation of Bud2p because GFP–Bud2p-dN40 was still properly localized to the bud neck (Supplemental Figure S4A). In addition, Bud2p-dN40 partially restored (~40%) the budding pattern abnormality of *bud2*Δ cells (Supplemental Figure S4B). We further investigated whether expression of the Bud2p-binding defective mutant Arf3p^{I33V} also impairs yeast invasive growth. We observed that the agar invasion defect seen in *arf3*Δ cells could be restored by *ARF3* and *ARF3^{L23V}* but not *ARF3^{I33V}* (Figure 3B). Of note, Arf3p^{I33V} was also unable to rescue the budding pattern abnormality observed in *arf3*Δ cells (Supplemental Figure S4C). Together these data demonstrate that an interaction between Arf3p and Bud2p is required for the proper function of these proteins in yeast invasive growth.

Accumulation of Bud1p-GTP prevents yeast invasive growth

Bud2p is a GAP that promotes the hydrolysis of GTP by Bud1p (Park *et al.*, 1993), and Bud5p acts as a GTP-exchange factor that catalyzes the binding of GTP to Bud1p (Chant *et al.*, 1991). Thus we examined whether the *bud1*Δ and *bud5*Δ mutants are also defective in agar invasion. Surprisingly, neither the *bud1*Δ nor *bud5*Δ mutant exhibited defects in invasive growth, suggesting that the

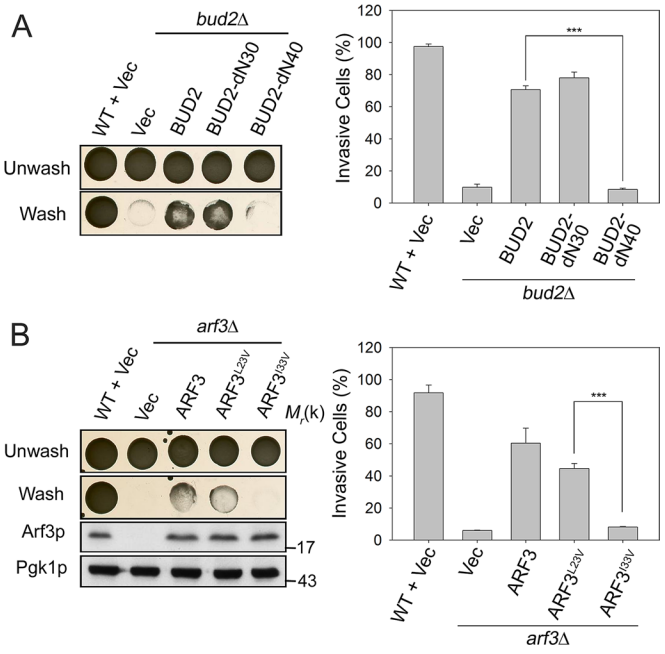

FIGURE 3: Arf3p interacts with Bud2p to regulate yeast invasive growth. (A) Expression of Bud2p-dN40 prevents yeast invasive growth in *bud2*Δ cells. Σ1278b yeast cells containing a *BUD2* deletion transformed with different forms of *BUD2* (full length, dN30, or dN40) were spotted onto YPD plates to examine agar penetration, and the percentage of invasive cells was quantified as described in *Materials and Methods*. (B) Expression of Arf3p^{I33V} reduces agar invasion in the *arf3*Δ mutant strain. Σ1278b yeast cells containing an *ARF3* deletion transformed with various *ARF3* alleles (wild type, L23V, and I33V) driven by the *ARF3* promoter were spotted onto YPD plates to examine agar penetration, and percentage of invasive cells was quantified. Protein extracts from the indicated strains were detected with anti-Arf3p and anti-Pgk1p (internal control). The data are reported as mean ± SD of three experiments. *** $p < 0.001$.

polarity module involved in bud-site selection functions differently in yeast invasive growth (Supplemental Figure S5A). Accordingly, overexpression of wild-type or inactive (GDP-bound) Bud1p^{K16N} did not affect invasive growth. However, overexpression of the constitutively active (GTP-bound) Bud1p^{G12V} significantly interfered with yeast invasive growth (Supplemental Figure S5B). This result suggests that overproduction of Bud1p-GTP could obstruct yeast invasive growth; therefore the defect in *arf3*Δ and *bud2*Δ cells is due to the accumulation of Bud1p-GTP, and depletion of *BUD1* may suppress the invasive growth defect seen in these cells. We generated *bud2bud1*Δ and *arf3bud1*Δ double-mutant strains to test this hypothesis and observed that deletion of *BUD1* in *arf3*Δ or *bud2*Δ cells significantly suppresses the defect in agar invasion (Figure 4A). Consistently, we also observed that decreasing Bud1p-GTP levels by deleting *BUD5* could suppress the agar invasion defect in *bud2*Δ cells (Supplemental Figure S5C). By contrast, *flo11bud1*Δ mutant cells, similar to *flo11*Δ cells, exhibit a defect in invasive growth. Of note, we found that deletion of *BUD1* in a *bud2*Δ strain completely restores invasive growth; deletion of *BUD1* in an *arf3*Δ strain, however, only partially restores it, suggesting that the accumulation of Bud1p-GTP is just part of Arf3p's role in invasive growth. Furthermore, we observed that overexpression of Bud1p and Bud1p^{G12V} caused an invasive growth defect in *arf3bud1*Δ and *bud2bud1*Δ cells, whereas Bud1p^{K16N}-overexpressing yeast maintained their agar invasion ability (Figure 4B).

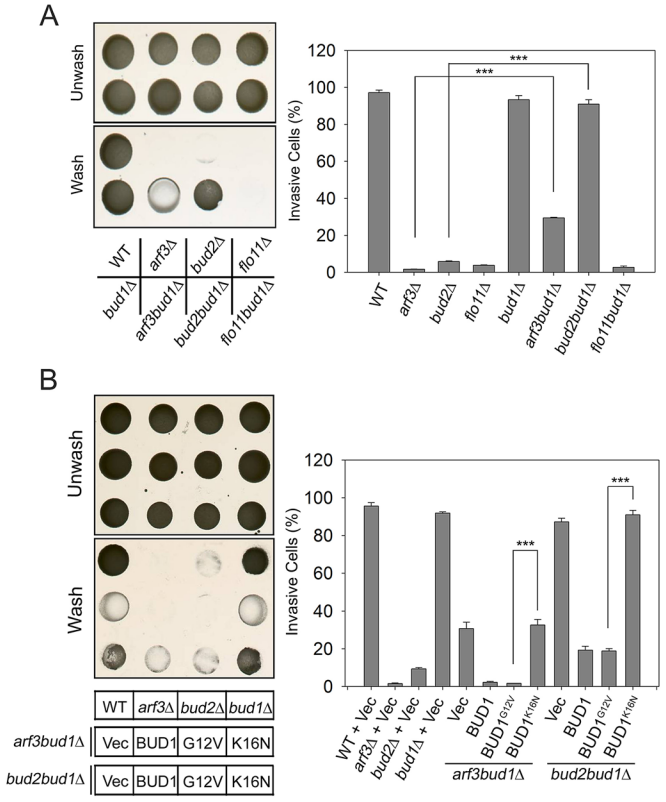

FIGURE 4: Accumulation of Bud1p-GTP prevents yeast invasive growth. (A) Additional depletion of *BUD1* suppresses the defect in agar invasion observed in *arf3*Δ or *bud2*Δ mutant cells. The indicated Σ1278b strains were spotted onto YPD plates and incubated for 3 d at 30°C. The plates were photographed before (top) and after (bottom) rinsing with water. Right, quantification of the percentage of invasive cells. (B) Expression of active Bud1p prevents agar invasion in *arf3bud1*Δ and *bud2bud1*Δ double-mutant cells. *arf3bud1*Δ or *bud2bud1*Δ double-mutant yeast Σ1278b cells transformed with a vector control and different alleles of *BUD1* (wild type, G12V, and K16N) were spotted onto YPD plates to examine agar penetration, and the percentage of invasive cells was quantified. Right, quantification of the percentage of invasive cells. Data are reported as the mean ± SD of three experiments. *** $p < 0.001$.

These data suggest that the inhibition of yeast invasive growth in *bud2*Δ and *arf3*Δ mutant cells occurs via the accumulation of Bud1p-GTP.

The GAP activity of Bud2p is required for invasive growth

Given that increased levels of Bud1p-GTP interfere with invasive growth, we hypothesized that the GAP activity of Bud2p is required for this process. To test this hypothesis, we first created a Bud2p GAP-defective mutant. GAP1^{IP4BP} is a GAP for Rap1, the mammalian homologue of Bud1p and has functional domains that are similar to those of Bud2p. Two point mutations in GAP1^{IP4BP}—GAP1^{IP4BP}-L484A and GAP1^{IP4BP}-R485Q—significantly impaired its GAP activity (Kupzig *et al.*, 2006). The L484 and R485 mutations in GAP1^{IP4BP} are equivalent to L681 and R682 in Bud2p (Supplemental Figure S6A). This leucine residue is highly conserved among members of the GAP family because it stabilizes the arginine finger, which is vital for its GAP activity (Kupzig *et al.*, 2006). To determine whether the L681A and R682Q mutations in Bud2p (Bud2p^{AQ}) cause defects in GAP activity, we immunoprecipitated HA-Bud2p and HA-Bud2p^{AQ} from yeast lysates and incubated them with recombinant [γ-^{32}P]GTP-bound GST-Bud1. The decrease in protein-bound radioactivity was measured and calculated as a measure of GTP hydrolysis. Bud2p^{AQ} showed a significantly reduced ability to promote Bud1p-GTP hydrolysis; thus Bud2p^{AQ} is indeed a GAP-defective mutant (Supplemental Figure S6B). We further demonstrated that expression of GAP-defective Bud2p^{AQ} could not rescue the defects in the axial budding pattern or invasive growth in *bud2*Δ cells (Supplemental Figure S6, C and D). Collectively these data indicate that the GAP activity of Bud2p is required for both types of yeast polarized growth.

The Arf3p–Bud2p interaction promotes Bud1p-GTP hydrolysis in vivo

Similar to *bud2*Δ, the loss of invasive growth in *arf3*Δ depends on the presence of *BUD1*, suggesting that the equilibrium of GTP- or GDP-bound Bud1p may be altered in *arf3*Δ cells. To quantify the levels of Bud1p-GTP in vivo, we used recombinant GST-Cdc42-GDP to specifically pull down Bud1p-GTP (Kozminski *et al.*, 2003). We first validated this pull-down assay using yeast cells overexpressing wild-type Bud1p, GTP binding-defective Bud1p^{K16N}, or GTP hydrolysis-deficient Bud1p^{G12V} protein. Bud1p^{G12V}, but not Bud1p^{K16N}, bound specifically to GST-Cdc42-GDP (Supplemental Figure S7), suggesting that this assay accurately reflects Bud1p-GTP levels in vivo. We therefore used this assay to quantify Bud1p-GTP in HA-Bud1p–expressing wild-type, *arf3*Δ, *bud2*Δ, and *bud5*Δ cells. Compared with wild-type cells, we observed a fourfold increase in Bud1p-GTP levels in both *arf3*Δ and *bud2*Δ cells (Figure 5A). Moreover, Bud1p-GTP was undetectable in *bud5*Δ cells. These data suggest that Arf3p is required for Bud1p-GTP hydrolysis in vivo. We next reintroduced mutant forms of Arf3p and Bud2p that are unable to interact with each other to determine whether the Arf3p–Bud2p interaction is required for the Bud1p GTP–GDP cycle. The level of Bud1p-GTP was significantly increased in *bud2*Δ cells expressing Bud2p-dN40 compared with those expressing HA-Bud2p (Figure 5B). Higher levels of Bud1p-GTP were consistently observed in vivo in the Bud2p-interaction–defective mutant Arf3p^{I33V} compared with wild-type Arf3p; this phenomenon, however, was not observed for Arf3p^{L23V}, which is capable of binding Bud2p (Figure 5C). Taken together, our results demonstrate that the Arf3p–Bud2p interaction is required to promote Bud1p-GTP hydrolysis in vivo.

Arf3p directly enhances Bud2p GAP activity in vitro

Given the direct interaction between Arf3p and Bud2p and the Arf3p requirement for Bud1p-GTP hydrolysis in vivo, we speculated that Arf3p could bind directly to Bud2p to promote Bud1p-GTP hydrolysis. Thus we measured the GAP activity of Bud2p in the presence of recombinant constitutively active Arf3^{Q71L} in vitro. HA-Bud2p was immunoprecipitated from yeast lysates and incubated with different amounts of purified Arf3^{Q71L}, and recombinant [γ-^{32}P] GTP-bound Bud1p was subsequently added to initiate the reaction. The GAP activity of Bud2p was measured as a function of the decrease in protein-bound radioactivity. Significantly, Bud2p-catalyzed Bud1 GTP hydrolysis was enhanced by Arf3^{Q71L} in a dose-dependent manner (Figure 6A). Next we performed kinetic measurement of GAP activity in the presence of Arf3^{Q71L} or Arf3^{T31N}. We found that Bud2p GAP activity was promoted by Arf3^{Q71L} but not by Arf3^{T31N} (Figure 6B). These data indicate that Arf3^{Q71L} directly promotes Bud2p GAP activity in vitro. We further examined the effect of the Arf3p–Bud2p interaction on Bud2p activity in vitro. Purified HA-Bud2p-dN40, which cannot bind Arf3p, exhibited impaired GAP activity compared with HA-Bud2p in vitro (Figure 6C). Moreover,

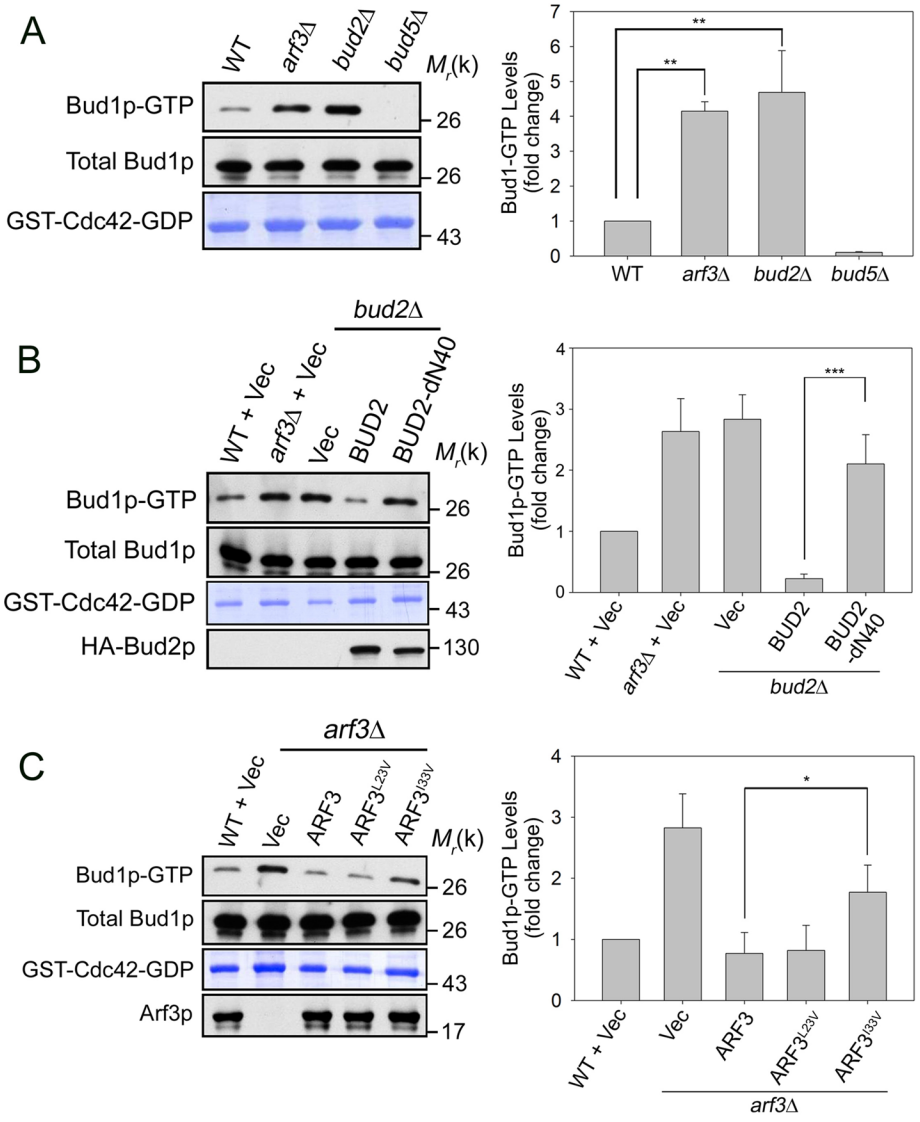

FIGURE 5: Bud2p interacts with Arf3p to enhance GAP activity leading to Bud1p-GTP hydrolysis in vivo. (A) Elevated Bud1p-GTP levels were detected in *arf3*Δ and *bud2*Δ mutant cells. Yeast lysates from the indicated Σ1278b strains expressing HA-Bud1p were prepared and analyzed to detect bound proteins using recombinant GST-Cdc42 purified from *E. coli*, together with prebinding with GDP as described in *Materials and Methods*. Right, quantitative analysis of active Bud1p. (B) Expression of Bud2p-dN40 in *bud2*Δ cells decreases content of Bud1p-GTP in vivo. Yeast lysates from the indicated Σ1278b strains expressing HA-Bud1p were prepared and analyzed to detect active Bud1p, as described in *Materials and Methods*. Right, quantitative analysis of active Bud1p. (C) Expression of Arf3p^{I33V} in *arf3*Δ cells increases cellular Bud1p-GTP levels in vivo. Yeast lysates from the indicated Σ1278b strains expressing HA-Bud1p were prepared and analyzed to detect active Bud1p. Right, quantitative analysis of active Bud1p. Data are reported as the mean ± SD of three experiments. *$p < 0.05$; **$p < 0.01$; ***$p < 0.001$.

unlike HA-Bud2, the GAP activity of HA-Bud2p-d40N was not enhanced by Arf3^{Q71L} (Figure 6D). Taken together, our results demonstrate that active Arf3p directly interacts with Bud2p to promote Bud2p GAP activity.

Arf3p facilitates the Bud2p–Bud1p association in vivo

A GAP cascade has been identified in the small GTPase Rab/Ypt family in which Ypt32p recruits and stabilizes Gyp1p, the GAP for Ypt1p, and regulates the progression of membrane trafficking (Rivera-Molina and Novick, 2009). The subcellular localization of Bud2p, however, is independent of Arf3p, thus differing from the Ypt GAP cascade. To further examine how activated Arf3p facilitates the GAP activity of Bud2p toward Bud1p, we examined the affinity of Bud2p for Bud1p in the presence and absence of Arf3p. We coexpressed HA-Bud2p and GFP-Bud1p (G12V or K16N) in wild-type or *arf3*Δ cells and immunoprecipitated HA-Bud2p to detect bound Bud1p. Our data indicated that Bud2p coprecipitated with Bud1p^{G12V} but not Bud1p^{K16N}; the association between Bud2p and Bud1p^{G12V}, however, was diminished in *arf3*Δ mutant cells (Figure 6E). In addition, we observed that Bud2p-dN40 exhibits decreased Bud1p^{G12V} binding in the presence of Arf3p (Figure 6F). Collectively these data suggest that Arf3p facilitates the interaction between Bud2p and Bud1p, thereby promoting Bud2p GAP activity.

Arf3p is activated by glucose depletion

Previous reports indicated that removal of glucose from the growth medium leads to constitutive invasion in haploid yeast (Cullen and Sprague, 2000). Thus we examined the effect of glucose on the invasiveness of haploid yeast cells and found that the removal of glucose (only yeast extract and peptone were present in the medium [YP]) caused constitutive invasion in wild-type yeast cells, in contrast to a glucose-containing medium (yeast extract/peptone/dextrose [YPD]), after incubation for 16 h (Figure 7A). Both *arf3*Δ and *bud2*Δ, but not *bud1*Δ, cells were constitutively defective in YP agar invasion (Figure 7A). The defect in agar invasion exhibited by *arf3*Δ cells was restored via expression of *ARF3* and *ARF3^{L23V}* but not of *ARF3^{Q71L}*, *ARF3^{T31N}*, and *ARF3^{I33V}* (Supplemental Figure S8A). Of interest, after glucose removal, Arf3p-mRFP and GFP-Bud2p showed dramatic polarization at the plasma membrane of elongated buds instead of being enriched at the bud neck in large-budded cells (Figure 7B). The polarized distribution of GFP-Bud2p and Arf3p-GFP in YP medium was not observably different in *arf3*Δ and *bud2*Δ cells (Supplemental Figure S8, B and C), indicating that intracellular targeting of Arf3p and Bud2p in response to glucose depletion is independent of their interaction.

To examine whether Arf3p activity could be affected by glucose depletion, we measured the amount of active Arf3p using recombinant GST-Afi1N to pull down Arf3p-GTP (Tsai *et al.*, 2008). GST-Afi1N specifically bound to active Arf3p^{Q71L} but not inactive Arf3p^{T31N} (Figure 8A). Using this assay, we observed an increase in Arf3p-GTP when yeast cells were grown in YP (Figure 8A). Of importance, we detected more Arf3p bound to Bud2p in response to glucose depletion (Figure 8B). Consistent with our data, we also observed that the level of Bud1p-GTP in wild-type cells was significantly

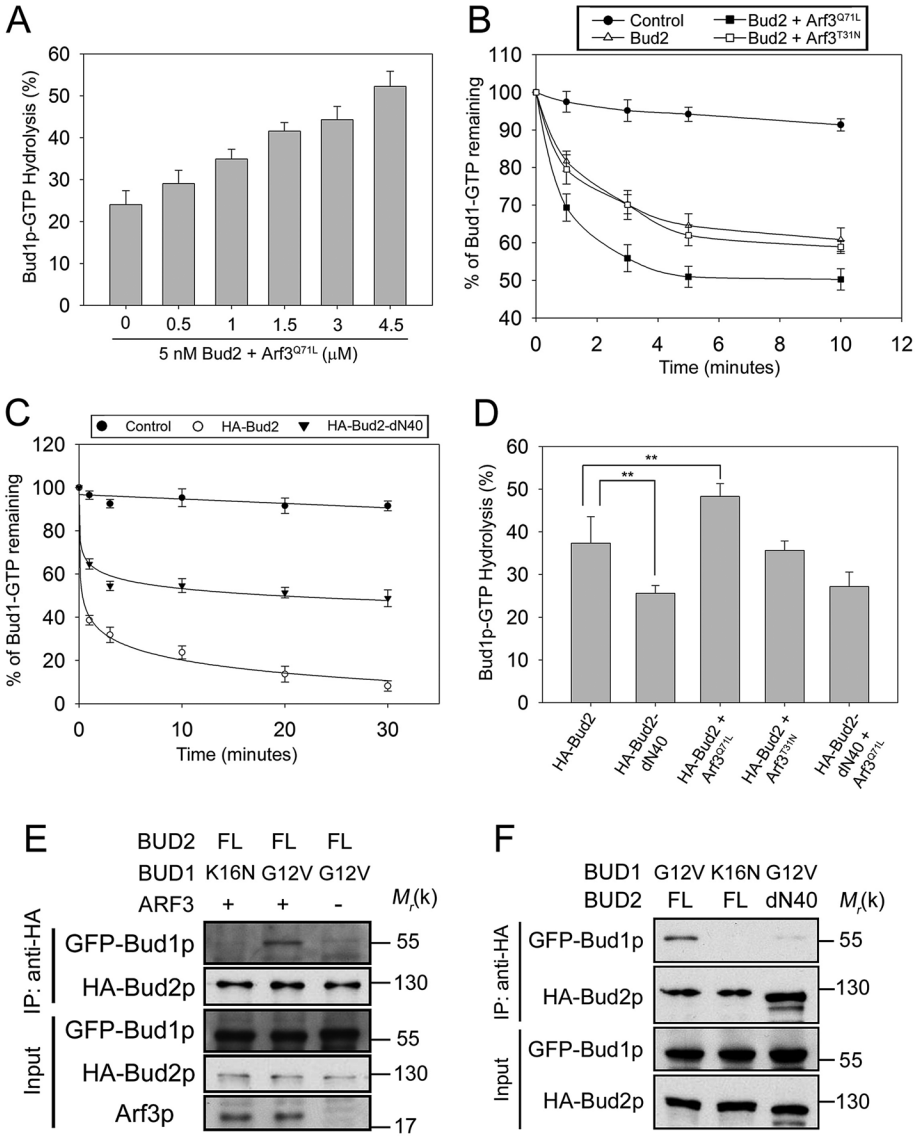

FIGURE 6: Interaction of Arf3p and Bud2p promotes Bud2p GAP activity, leading to Bud1p GTP hydrolysis. (A) Arf3p^{Q71L} enhances Bud2p GAP activity in a dose-dependent manner. Purified recombinant GST-Bud1 (1 μM) loaded with [γ-^{32}P]GTP was incubated with purified HA-Bud2p (5 nM) alone or in the presence of recombinant His-Arf3^{Q71L} at 30°C for 10 min. Samples were collected, and protein-bound radioactivity was detected using a nitrocellulose filter–binding assay. (B) Enhancement of Bud2p GAP activity by Arf3p^{Q71L}. [γ-^{32}P]GTP bound to recombinant GST-Bud1 was incubated with a buffer control or HA-Bud2p (5 nM) with or without 1 μM His-Arf3^{Q71L} or His-Arf3^{T31N} for the indicated time periods. After incubation, the hydrolysis of [γ-^{32}P]GTP bound to GST-Bud1 was assayed by measuring radioactivity. (C) Compared to full-length Bud2p, Bud2p-dN40 shows decreased GAP activity. The GAP activity of purified Bud2p or Bud2p-dN40 (50 nM) was assayed using purified GST-Bud1 with bound [γ-^{32}P]GTP as a substrate, as described in *Materials and Methods*. The results are representative of three experiments. (D) The GAP activity of Bud2p-dN40 is not enhanced in the presence of Arf3p^{Q71L}. Purified recombinant GST-Bud1 (1 μM) loaded with [γ-^{32}P]GTP was incubated with 5 nM HA-Bud2p or HA-Bud2p-dN40 with or without 1 μM Arf3^{Q71L} or Arf3^{T31N} for 10 min. Samples were collected to measure protein-bound radioactivity. (E) Arf3p potentiates the association between Bud2p and Bud1p. Different forms of GFP-Bud1p (G12V or K16N) were coexpressed with HA-Bud2p in wild-type or *arf3*Δ yeast Σ1278b cells. As described in *Materials and Methods*, HA-Bud2p was immunoprecipitated with an anti-HA antibody, and the bound proteins were assayed for the presence of different forms of Bud1p. (F) Bud2p-dN40 associates with Bud1p more weakly than Bud2p does. Different forms of GFP-Bud1p (G12V or K16N) were coexpressed with full-length (FL) HA-Bud2p or HA-Bud2p-dN40 in yeast Σ1278b cells. HA-Bud2p was immunoprecipitated with an anti-HA antibody, and the bound proteins were detected with antibodies against GFP. Data are reported as the mean ± SD of the percentage of [γ-^{32}P]GTP hydrolysis ($n = 3$). $^{**}p < 0.01$.

decreased in response to glucose depletion (Figure 8C). These data suggest that glucose removal activates Arf3p and promotes Arf3p-Bud2p interaction and GTP hydrolysis of Bud1p to initiate yeast invasive signaling.

Glucose depletion induces Arf3p activation via a Yel1p-independent pathway

Yel1p is the only known GEF for Arf3p (Gillingham and Munro, 2007). Therefore it is surprising that the disruption of *YEL1* did not affect yeast invasive growth (Figure 9A). Furthermore, even though active Arf3p in *yel1*Δ cells was significantly reduced (Gillingham and Munro, 2007; Tsai *et al.*, 2008), the interaction between Arf3p and Bud2p remained at a similar level in the absence of Yel1p (Figure 9B). These data suggest that Arf3p activation during invasive growth is independent of Yel1p. Previous studies showed that Arf3p proteins are recruited to the plasma membranes in their GTP-bound form (Huang *et al.*, 2003) and loss of *YEL1* results in the mislocalization of Arf3p to the cytosol (Gillingham and Munro, 2007). We sought to further examine the localization of Arf3p in *yel1*Δ under glucose depletion. Consistent with previous report, the majority of Arf3p is in the cytosol, indicating a decrease of Arf3p-GTP in *yel1*Δ; we still observed, however, an increase in Arf3p polarization on the plasma membrane upon glucose deprivation in the absence of Yel1p (Figure 9C). We obtained additional evidence for this phenomenon by measuring Arf3p activity in *yel1*Δ cells and found that glucose depletion could still stimulate Arf3p activation in *yel1*Δ cells (Figure 9D). Together these data indicate that the activation of Arf3p during invasive growth does not occur through the GEF activity of Yel1p. We also examined whether other Arf-GEFs, *GEA1, GEA2,* or *SYT1*, might be involved in Arf3p activation for invasive growth (Zakrzewska *et al.*, 2003; Chen *et al.*, 2010). Similar to the *yel1* mutant, *yel1gea1*Δ, *yel1gea2*Δ, and *yel1syt1*Δ Σ1278b cells remained at a similar level of invasive growth under glucose depletion (Supplemental Figure S9), suggesting that there is an unknown Arf3p GEF that activates Arf3p under glucose depletion–stimulated invasive growth.

DISCUSSION

In this study, we identified a novel role for Arf3p in yeast invasive growth. We showed that Arf3p directly interacts with Bud2p and regulates its GAP activity toward Bud1p by enhancing the association between Bud2p and Bud1p. Finally, we showed that under

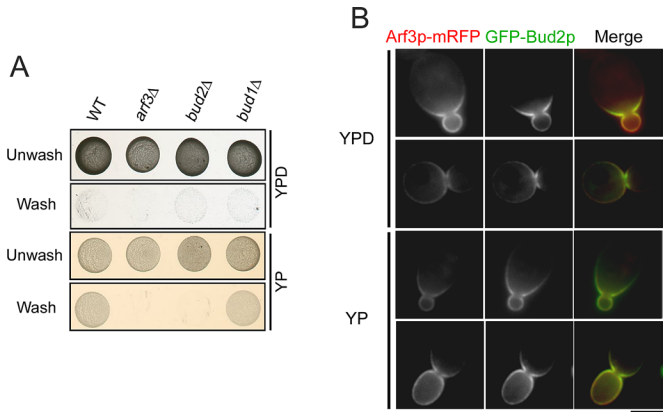

FIGURE 7: Arf3p is activated by glucose depletion. (A) Arf3p and Bud2p are required for yeast invasion during glucose depletion. Equal concentrations of wild-type, *arf3*Δ, *bud2*Δ, and *bud1*Δ yeast Σ1278b cells were spotted onto YPD (2% glucose) or YP (0% glucose) plates and incubated for 16 h at 30°C. The plates were photographed before (top) and after (bottom) rinsing with water. (B) GFP-Bud2p and Arf3p-mRFP exhibit a polarized distribution in the elongated bud cell under glucose depletion. Wild-type yeast Σ1278b cells were cotransformed with *GFP-BUD2*/pVT101U and *ARF3-mRFP*/pHS12. The yeast were grown in rich media with (YPD) or without (YP) glucose for 16 h and observed via fluorescence microscopy. Scale bars, 5 μm.

glucose depletion–stimulated invasive growth, Arf3p activation is stimulated through an unidentified GEF other than Yel1p. Thus this novel nutrient-stimulated mechanism for the activation of Arf3p and Bud2p provides a functional connection between members of different subfamilies of small GTPases, Arf3p and Bud1p, for the regulation of invasive growth.

The Bud1p GTPase module composed of Bud1p, the GAP Bud2p, and the GEF Bud5p is a critical regulator of bud site selection linking to polarity establishment during yeast vegetative growth, and the mechanism of its action has been well characterized (Park and Bi, 2007). Bud1p-GTP interacts with Cdc24p and guides it to the presumptive bud site, where Bud2p is localized. The Bud2p-activated hydrolysis of Bud1p-GTP then results in the dissociation of Cdc24p from Bud1p. Cdc24p free of Bud1p subsequently catalyzes the conversion of Cdc42p-GDP to Cdc42p-GTP to mediate actin cytoskeleton reorganization and lead to the development of cellular polarity (Butty *et al.*, 2002). Our results indicate that Arf3p modulates Bud1p activity via Bud2p; therefore it is tempting to assume that Arf3p affects Cdc24p polarization via Bud1p activation. Cdc24p is the Cdc42p GEF, and its polarized localization is critical for proper activation of Cdc42p and cytoskeleton reorganization (Park *et al.*, 2002). We hypothesize that Arf3p interacts with Bud2p to promote Bud1p-GTP hydrolysis, which, in turn, releases Cdc24p to activate Cdc42p and leads to invasive growth. Similarly, inhibition of the mammalian Arf3p homologue, Arf6, was reported to abolish the polarized recruitment of mammalian Cdc42 to the leading edge of cultured cells (Osmani *et al.*, 2010).

Invasive growth of *S. cerevisiae* has been used as a model system for studying the filamentous growth of pathogenic yeast and nutrient-stimulated cellular responses, including signaling transduction, cell cycle control, polarized growth, and cell survival. The formation of hyphae in the human pathogen *C. albicans* is critical during the infection process (Sudbery, 2011). Of note, *C. albicans bud1*Δ/Δ and *bud2*Δ/Δ strains are defective in the formation of filamentous hyphae (Hausauer *et al.*, 2005). In addition, AgRsr1p/Bud1p was also reported to be a key regulator of hyphal growth guidance in the model fungus *Ashbya gossypii* (Bauer *et al.*, 2004). We also observed that Bud1p and Bud2p activation is important for the invasive growth of *S. cerevisiae*. Moreover, our preliminary data showed that *C. albicans* failed to generate extended hyphae when two copies of the *CaARF3* gene were deleted. Therefore we speculate that both Arf3p and Bud2p are required for the invasive growth of *S. cerevisiae* and hyphal guidance in *C. albicans*, suggesting that Arf3p may play an important role during the infection process of microbial pathogens. Of interest, Arf6, the mammalian homologue of yeast Arf3p, is known to be involved in cell adhesion, migration, and metastasis (Sabe, 2003). In addition, previous studies found that the mammalian Bud1p homologue, Rap1, regulates the dynamics of cell adhesion (Bos *et al.*, 2001). Therefore our studies of Arf3p suggest that Arf6 may regulate Rap1 activity associated with mammalian cell adhesion, migration, and invasion.

Alteration of subcellular protein localizations under different physiological conditions is critical for proper protein function. On glucose depletion, Arf3p and Bud2p become highly colocalized at the plasma membrane of elongated daughter cells, in contrast to their partial colocalization observed in normal medium. Similarly, our results show that although both *arf3*Δ and *bud2*Δ cells exhibit an abnormal budding pattern during polarized growth, the randomness seen in *bud2*Δ cells is much more severe than that in *arf3*Δ cells. Taken together, these data indicate that Arf3p is not the major regulator of Bud2p activity during polarized growth; Arf3p is further activated, however, upon glucose depletion and becomes the main regulator of Bud2p activity during yeast invasion. This speculation is further supported by our observation that Bud2p-dN40, like *arf3*Δ, only exhibits a mild budding pattern abnormality; Bud2p-dN40, however, is completely unable to support invasive growth. Therefore multiple mechanisms must be used by Bud2p to establish bud site selection linking to cell polarity under different physiological conditions. Whereas deletion of *BUD1* in a *bud2*Δ strain completely restores invasive growth, deletion of *BUD1* in an *arf3*Δ strain only partially restores it. These results suggest that the regulation of Bud2p GAP activity toward Bud1p is just part of Arf3p's role in invasive growth. Lsb5p was reported to interact with Arf3p and actin-binding protein Sla1p for regulating membrane trafficking events with the endocytic machinery (Costa *et al.*, 2005). It was shown that deletion of *SLA1* in yeast leads to loss of nitrogen starvation–induced filamentous growth (Wu and Jiang, 2005). A previous study also showed that altered levels of Arf3p affect plasma membrane phosphatidylinositol 4,5-bisphosphate levels and correlate with changes in numbers of endocytic events (Smaczynska-de *et al.*, 2008). The processes by which activation of Arf3p fosters invasive growth need to be investigated further. Therefore Arf3p must use multiple effectors to regulate invasive growth in yeast.

GTP binding is necessary for the activation of small GTPases and is tightly regulated by GEFs and GAPs. Although Yel1p is the only known Arf3p GEF (Gillingham and Munro, 2007; Smaczynska-de *et al.*, 2008), we found that the deletion of *YEL1* in yeast did not reduce invasive growth and Yel1p is not required for Arf3p activation in response to glucose depletion. These data indicate that there is an unknown Arf3p GEF that activates Arf3p during invasive growth. Consistent with this proposal, previous studies also suggested that Yel1p is not the only GEF for Arf3p, because some Arf3p can still localize to the plasma membrane in *yel1*Δ cells (Gillingham and Munro, 2007; Tsai *et al.*, 2008). Of note, our results indicate that the known Arf-GEFs Gea1p, Gea2p, and Syt1p are not responsible for Arf3p activation during invasive growth. Furthermore, we found that lack of Gts1p, the only known Arf3p GAP (Gillingham and Munro, 2007; Smaczynska-de *et al.*, 2008), also did not reduce invasive growth of

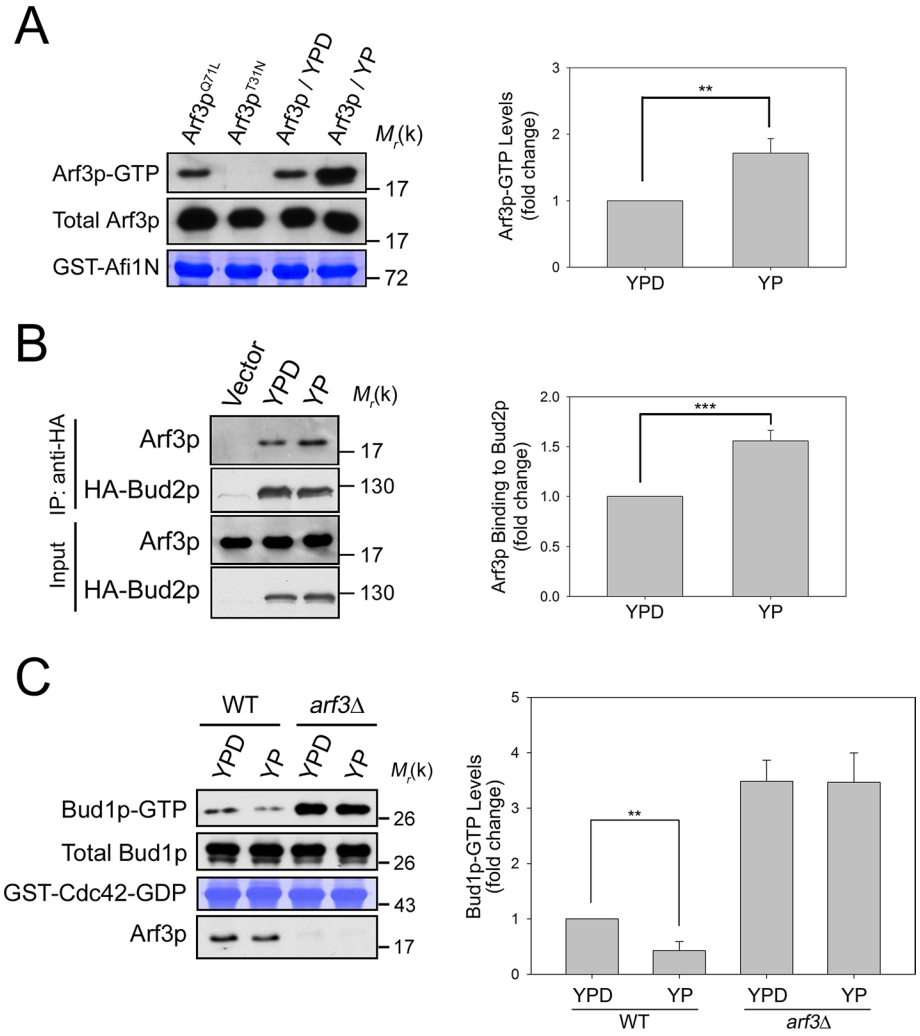

FIGURE 8: Glucose depletion induces Arf3p activation to promote Bud1p-GTP hydrolysis. (A) Active forms of Arf3p are elevated under glucose depletion. Σ1278b yeast cells growing in rich medium containing 2% glucose were transferred to rich medium containing no glucose (YD) or rich medium containing 2% glucose (YPD) for 16 h. After the indicated time periods, cellular Arf3p-GTP levels were detected with recombinant GST-Afi1N purified from *E. coli*, as described in *Materials and Methods*. Bottom, quantitative analysis of active Arf3p. Data are reported as the mean ± SD of three experiments. $^{**}p < 0.01$ (B) Glucose depletion enhances the Arf3p-Bud2p interaction. As described *Materials and Methods*, Σ1278b yeast cells cultured in rich medium with (YPD) or without glucose (YP) were harvested; HA-Bud2p was immunoprecipitated using an anti-HA antibody, and bound Arf3p proteins were assayed by immunoblotting. Data are reported as the mean ± SD of three experiments. $^{***}p < 0.001$. (C) Glucose depletion enhances Bud1p-GTP hydrolysis. As described in *Materials and Methods*, wild-type and *arf3*Δ Σ1278b yeast cells expressing HA-Bud1p cultured in rich medium with (YPD) or without glucose (YP) were harvested and analyzed to detect active Bud1p. Data are reported as the mean ± SD of three experiments. $^{**}p < 0.01$.

yeast (our unpublished results). Thus the activation of small GTPases is regulated by unknown GEFs and GAPs during glucose depletion–induced invasive growth.

In this study, we identify Arf3p as an upstream regulator of Bud2p and propose the existence of a novel small GTPase cascade, Arf3p-Bud2p-Bud1p, which orchestrates the polarity development during invasive growth. During vegetative growth, Arf3p is only responsible for partial activation of Bud2p, leading to yeast axial budding. A portion of activated Arf3p, however, stimulated by glucose depletion, plays a crucial role in attenuating Bud1p activation by promoting the GAP activity of Bud2p involved in invasive growth (Figure 10). After activation via an unidentified GEF under glucose depletion conditions, Arf3p directly binds to Bud2p to promote Bud1p-GTP hydrolysis, which leads to Cdc24p disassociation and Cdc42p activation. Thus we propose the existence of a hierarchical GTPase cascade involving Arf3p-Bud1p that 1) modulates a unique effector via controlling regulators of Bud1p and 2) coordinates signaling by glucose depletion during yeast invasive growth. Therefore our results imply that Arf3p GTPases can regulate two different processes by recruiting process-specific effectors. Further studies are required to reveal the full spectrum of Arf3p activation mechanisms under glucose-limiting–induced invasive growth.

MATERIALS AND METHODS

Plasmids, strains, and yeast culture

Standard protocols were used to generate Σ1278b yeast strains via homologous recombination (Longtine *et al.*, 1998). All of the yeast *ARF3* plasmids used here encode Arf3p constructs driven by the native *ARF3* promoter. The plasmids and yeast strains used are listed in Supplemental Tables S1 and S2 (Vernet *et al.*, 1987; Gietz and Sugino, 1988; Sikorski and Hieter, 1989). For glucose depletion, Σ1278b yeast cells were cultured in YPD overnight, washed three times with double-distilled H_2O, recultured in YP medium (or spotted on YP agar plates), and incubated for 16 h.

In vitro binding assay

Escherichia coli strain BL21 (DE3; Novagen, La Jolla, CA) was transformed with plasmids including pET32a-ARF3 (Q71L or T31N), pGEX4T-1, and pGEX4T-1 containing various BUD2 fragments, as shown in Figure 1D. After induction with 500 μM isopropyl-β-D-thiogalactoside at 16°C for 8 h, GST fusion proteins or His-tagged proteins were purified from *E. coli* lysates using glutathione–Sepharose 4B (GE Healthcare Amersham, Piscataway, NJ) or nickel affinity resin (Qiagen, Valencia, CA), respectively, according to the manufacturer's instructions. In pull-down assays, GST or GST-Bud2 fragments were immobilized on glutathione agarose beads and incubated with His-Arf3 (Q71L or T31N) in binding buffer (50 mM Tris-HCl, pH 7.5, 150 mM NaCl, 1% Triton X-100, 1 mM dithiothreitol [DTT], and 10 mM $MgCl_2$) for 2 h at 4°C. The beads were washed three times with 1 ml of binding buffer. Bound proteins were then analyzed by Western blotting using anti-His monoclonal antibodies (BD Biosciences, La Jolla, CA).

Yeast two-hybrid assay

The yeast strain YEM1α was cotransformed with different combinations of bait (pEG202) and prey (pACT2) plasmids (Gyuris *et al.*, 1993). The interactions between the bait and prey plasmids were observed

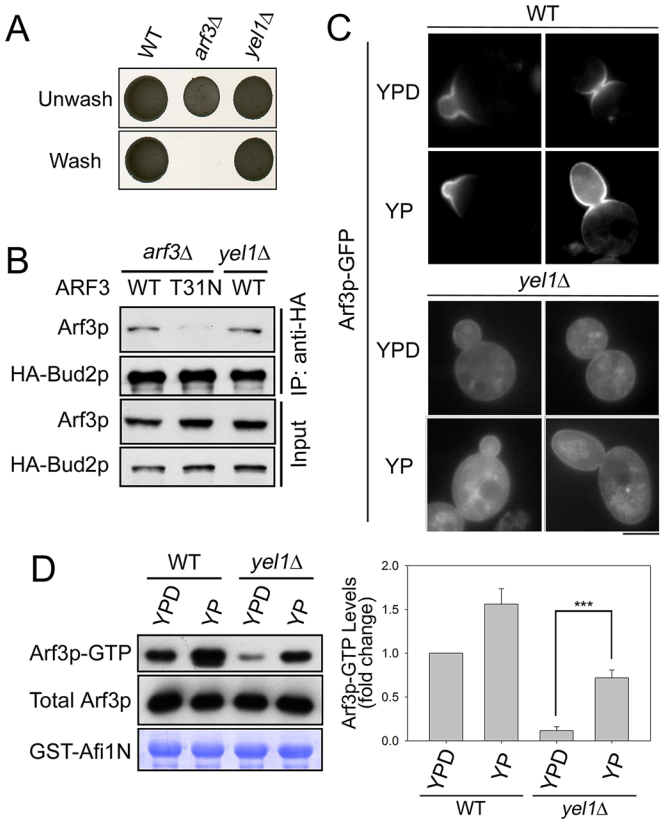

FIGURE 9: Glucose depletion induces Arf3p activation via a Yel1p-independent pathway. (A) Yel1p is not required for agar invasion. Equal concentrations of wild-type, *arf3*Δ, and *yel1*Δ Σ1278b yeast cells were spotted onto YPD plates and incubated for 3 d at 30°C. The plates were photographed before (top) and after (bottom) rinsing with water. (B) Arf3p associates with Bud2p in *yel1*Δ cells. Arf3p was expressed in *arf3*Δ and *yel1*Δ Σ1278b yeast cells with HA-Bud2p. As described in *Materials and Methods*, HA-Bud2p was immunoprecipitated with an anti-HA antibody, and the bound proteins were assayed for the presence of different forms of Arf3p. (C) Disruption of *YEL1* in yeast cells shows signals that polarize Arf3p-GFP to the bud tip in the absence of glucose. *ARF3-GFP*/YCplac111 was transformed into wild-type and *yel1*Δ Σ1278b yeast cells. Yeast cells treated with or without glucose for 16 h were observed by fluorescence microscopy. Scale bars, 5 μm. (D) Active forms of Arf3p are elevated in *yel1*Δ cells upon glucose depletion. Wild-type and *yel1*Δ Σ1278b yeast cells expressing *ARF3* and grown in rich medium containing 2% glucose were switched to rich medium containing no carbon source or rich medium containing 2% glucose for 16 h. After the indicated time periods, cellular Arf3p-GTP levels were detected with recombinant GST-Afi1N purified from *E. coli* as described in *Materials and Methods*. Right, quantitative analysis of active Arf3p. Data are reported as the mean ± SD of three experiments. ***$p < 0.001$.

using a β-galactosidase assay on His– Leu– plates containing 80 mg/l X-Gal.

Immunoprecipitation

Σ1278b yeast cells were disrupted with glass beads in extraction buffer (phosphate-buffered saline [PBS] containing 1 mM DTT, 5 mM $MgCl_2$, and protease inhibitors). The extracts were cleared via centrifugation at 4000 rpm for 10 min. Agarose beads conjugated with a monoclonal anti-HA antibody (mouse monoclonal anti–HA agarose antibody; Sigma-Aldrich, St. Louis, MO) were added to the cleared extracts and incubated at 4°C for 2 h. The beads were washed three times with wash buffer (extraction buffer containing 0.5% NP-40), and the bound complexes were eluted with sample buffer. The bound proteins were subjected to SDS–PAGE and analyzed via Western blotting.

Microscopy

All images of living cells containing GFP-tagged or mRFP-tagged proteins were obtained after growth in synthetic medium to mid–log phase. Fluorescence microscopy was performed with a Zeiss Axioskop microscope (Carl Zeiss, Jena, Germany) equipped with a CoolSNAP FX camera (Photometrics, Tucson, AZ). Cells were viewed at a magnification of 100×. For all microscopic examinations, the exposure times and image processing procedures were identical for each sample within an experiment. The light levels were scaled equivalently among all samples within an experiment when the images were exported from the imaging software and when they were subsequently processed with Photoshop (Adobe, San Jose, CA). Only the light level min/max settings were adjusted for clarity.

Calcofluor white staining

To stain bud scars, Σ1278b yeast cells were grown overnight to the stationary phase. The cells were fixed with 3.7% formaldehyde for 1 h and stained with 1 μg/ml Calcofluor White (Sigma-Aldrich) as described previously (Huang *et al.*, 2003). Stained cells were photographed and quantified via fluorescence microscopy. A minimum of 100 cells was quantified for each experiment.

Subcellular fractionation

Σ1278b yeast cells expressing *ARF3*, *ARF3*^{L23V}, and *ARF3*^{I33V} were harvested and washed once in 10 mM NaN_3-containing buffer. The cells were incubated with lyticase in 1.2 M sorbitol-containing potassium phosphate buffer to form spheroplasts. The spheroplasts were disrupted by passing them through a 26-gauge needle. The cell lysate was then cleared by centrifugation at 600 × *g* for 5 min to remove debris and unbroken cells. The cleared lysate was next subjected to velocity centrifugation at 13,000 × *g* for 10 min to generate a pellet fraction (P13) and the supernatant fraction (S13). Equal proportions of each fraction were subjected to SDS–PAGE and analyzed via Western blotting using antibodies against Arf3p, Pma1p (plasma membrane marker), and Pgk1p (cytosol marker).

Invasive growth assays

The haploid cell invasive assay was performed as described previously (Lo and Dranginis, 1998; Guldal and Broach, 2006). Equal concentrations of Σ1278b yeast cells were spotted onto YPD medium. After incubation for 3 d at 30°C, cells that penetrated the agar were examined after washing cells off the agar surface with water. The samples were photographed before and after washing with a stream of water. To perform a quantitative agar invasion assay, agar blocks containing yeast colonies (before and after washing) were excised and placed into microcentrifuge tubes. Elution buffer containing 0.5 M sodium acetate (pH 7.0) and 1 mM EDTA (pH 8.0) was added, and the tubes were incubated at 55°C for 20 min until the agar blocks were completely dissolved. The yeast cell numbers were examined by measuring OD_{600} values to obtain total cell numbers before and after washing with water. The percentage of invasive cells observed after washing with water was determined as OD_{600} unit after washing/OD_{600} unit before washing × 100%. The data are reported as the mean ± SD of three experiments.

GAP activity assays

The Bud2p GAP activity assay was performed essentially as described previously (Park *et al.*, 1993). Briefly, GAP activity was assayed by measuring [γ-^{32}P]GTP after a single round of hydrolysis of

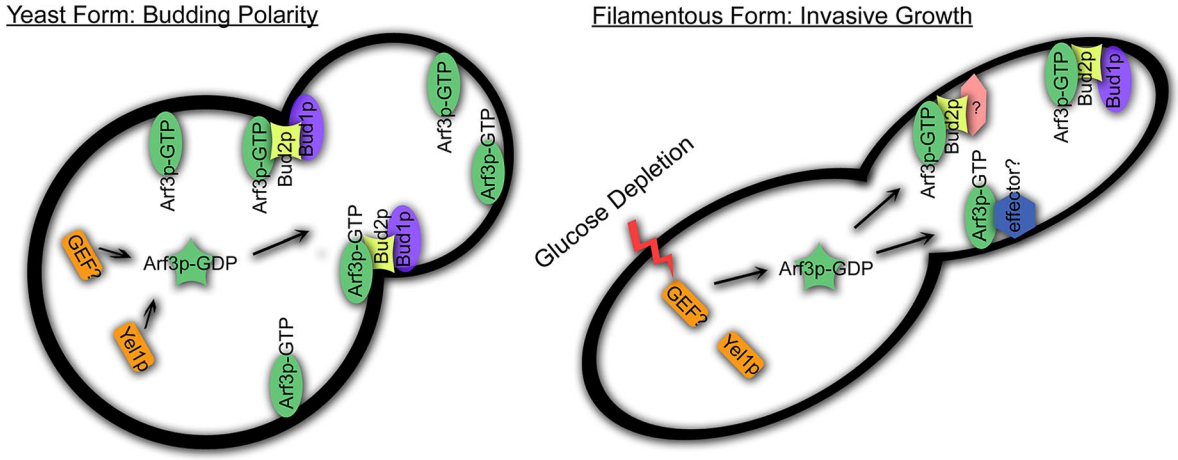

FIGURE 10: Model for the roles of Arf3p in budding polarity and yeast invasion. During polarized growth, Arf3p is activated through the recruitment of Yel1p or another redundant GEF to the bud neck (left). When Arfp3-GTP interacts with the N-terminus of Bud2p, Bud2p may strongly associate with Bud1p and efficiently promote GTP hydrolysis activity of Bud1p. Once Bud1p is converted into the inactivated GDP-bound form, it may activate and couple with a downstream Cdc42p GTPase module to maintain budding polarity. Under glucose depletion, an unidentified GEF, other than Yel1p, will be triggered to activate Arf3p (right). After its activation, Arf3p directly binds to Bud2p and promotes Bud1p-GTP hydrolysis. Thus the regeneration of Bud1p-GDP by Bud2p GAP activity via the cooperation of Arf3p may facilitate yeast invasive growth. Arf3p may also alter other, unidentified effectors that regulate yeast invasive growth.

Bud1-bound GTP by Bud2p. Recombinant GST-Bud1 was incubated in exchange buffer (PBS containing 1 mM EDTA, 0.5 mM $MgCl_2$, and 1 mM DTT) with [γ-^{32}P]GTP for 25 min at 30°C. HA-Bud2p or HA-Bud2p-dN40 was purified from Σ1278b yeast lysates and coincubated with GST-Bud1 with [γ-^{32}P]GTP loading at different time points. The reactions were terminated by increasing the $MgCl_2$ content (5 mM final concentration), and the samples were filtered through a 0.45-μm nitrocellulose membrane. The remaining Bud1-bound radioactivity was detected with a scintillation counter. In the Arf3p-related GAP activity assay, recombinant Arf3, Arf3^{Q71L}, or Arf3^{T31N} was purified and preincubated with HA-Bud2p or HA-Bud2p-dN40 for 1 h at 4°C. Data are reported as the mean ± SD of three experiments.

Active Bud1p pull-down assay

The activation of Bud1p was assayed using a novel pull-down assay. Three Bud1p alleles (wild type, G12V, and K16N) were tagged with HA and ectopically expressed in *bud1*Δ cells. Transformed yeast cells of Σ1278b were lysed with glass beads at 4°C in lysis buffer (PBS containing 1 mM DTT, 5 mM $MgCl_2$, 0.2% NP-40, and protease inhibitors [1 μg/ml aprotinin, 1 μg/ml leupeptin, 1 μg/ml pepstatin, 1 μM benzamidine, and 1 mM phenylmethylsulfonyl fluoride (PMSF)]). The lysates were centrifuged at 4000 rpm for 5 min, and the clarified lysates were incubated with 5 μg of GST-Cdc42-GDP bound to glutathione–Sepharose beads (GE Healthcare). The beads were washed three times with lysis buffer, and the bound proteins were eluted with sample buffer. The samples were assayed for presence of Bud1p by Western blotting.

To pull down Bud1p-GTP, yeast cells overexpressing HA-Bud1p under the control of the *ADH1* promoter were lysed, and bound proteins were analyzed as described.

Active Arf3p pull-down assay

Three Arf3p alleles (wild type, Q71L, or T31N) were ectopically expressed in wild-type cells. Σ1278b yeast cells expressing *ARF3* were grown in rich medium containing 2% (YPD) or 0% (YP) glucose and lysed with glass beads at 4°C in lysis buffer (PBS containing 1 mM DTT, 2 mM $MgCl_2$, and protease inhibitors [1 μg/ml aprotinin, 1 μg/ml leupeptin, 1 μg/ml pepstatin, 1 μM benzamidine, and 1 mM PMSF]). The lysates were centrifuged at 3000 rpm for 5 min, and the clarified lysates were incubated with 5 μg of GST-Afi1N bound to glutathione–Sepharose beads (GE Healthcare). The beads were washed three times with lysis buffer containing 0.2% Triton X-100, and the bound proteins were eluted with sample buffer. The samples were assayed for the presence of Arf3p by Western blotting.

ACKNOWLEDGMENTS

We thank Hugh R. B. Pelham, Kai Simons, and Roger Y. Tsien for providing the expression plasmids. We also thank Joel Moss and Randy Haun for their critical review of the manuscript. This work was supported by grants from the National Science Council of Taiwan (NSC-100-2320-B-002-101-MY3) and Yung-Shin Biomedical Research Funds (YSP-86-019) awarded to F.-J.L.

REFERENCES

Bauer Y, Knechtle P, Wendland J, Helfer H, Philippsen P (2004). A Ras-like GTPase is involved in hyphal growth guidance in the filamentous fungus *Ashbya gossypii*. Mol Biol Cell 15, 4622–4632.

Bender A (1993). Genetic evidence for the roles of the bud-site-selection genes BUD5 and BUD2 in control of the Rsr1p (Bud1p) GTPase in yeast. Proc Natl Acad Sci USA 90, 9926–9929.

Bos JL, de Rooij J, Reedquist KA (2001). Rap1 signalling: adhering to new models. Nat Rev Mol Cell Biol 2, 369–377.

Butty AC, Perrinjaquet N, Petit A, Jaquenoud M, Segall JE, Hofmann K, Zwahlen C, Peter M (2002). A positive feedback loop stabilizes the guanine-nucleotide exchange factor Cdc24 at sites of polarization. EMBO J 21, 1565–1576.

Chant J, Corrado K, Pringle JR, Herskowitz I (1991). Yeast BUD5, encoding a putative GDP-GTP exchange factor, is necessary for bud site selection and interacts with bud formation gene BEM1. Cell 65, 1213–1224.

Chavrier P, Menetrey J (2010). Toward a structural understanding of arf family:effector specificity. Structure 18, 1552–1558.

Chen KY, Tsai PC, Hsu JW, Hsu HC, Fang CY, Chang LC, Tsai YT, Yu CJ, Lee FJ (2010). Syt1p promotes activation of Arl1p at the late Golgi to recruit Imh1p. J Cell Sci 123, 3478–3489.

Costa R, Ayscough KR (2005). Interactions between Sla1p, Lsb5p and Arf3p in yeast endocytosis. Biochem Soc Trans 33, 1273–1275.

Costa R, Warren DT, Ayscough KR (2005). Lsb5p interacts with actin regulators Sla1p and Las17p, ubiquitin and Arf3p to couple actin dynamics to membrane trafficking processes. Biochem J 387, 649–658.
Cullen PJ, Sprague GF Jr (2000). Glucose depletion causes haploid invasive growth in yeast. Proc Natl Acad Sci USA 97, 13619–13624.
Cullen PJ, Sprague GF Jr (2002). The roles of bud-site-selection proteins during haploid invasive growth in yeast. Mol Biol Cell 13, 2990–3004.
Cullen PJ, Sprague GF Jr (2012). The regulation of filamentous growth in yeast. Genetics 190, 23–49.
D'Souza-Schorey C, Chavrier P (2006). ARF proteins: roles in membrane traffic and beyond. Nat Rev Mol Cell Biol 7, 347–358.
Donaldson JG, Jackson CL (2011). ARF family G proteins and their regulators: roles in membrane transport, development and disease. Nat Rev Mol Cell Biol 12, 362–375.
Gietz RD, Sugino A (1988). New yeast-*Escherichia coli* shuttle vectors constructed with in vitro mutagenized yeast genes lacking six-base pair restriction sites. Gene 74, 527–534.
Gillingham AK, Munro S (2007). Identification of a guanine nucleotide exchange factor for Arf3, the yeast orthologue of mammalian Arf6. PLoS One 2, e842.
Gimeno CJ, Ljungdahl PO, Styles CA, Fink GR (1992). Unipolar cell divisions in the yeast *S. cerevisiae* lead to filamentous growth: regulation by starvation and RAS. Cell 68, 1077–1090.
Guldal CG, Broach J (2006). Assay for adhesion and agar invasion in *S. cerevisiae*. J Vis Exp 1, e64.
Gyuris J, Golemis E, Chertkov H, Brent R (1993). Cdi1, a human G1 and S phase protein phosphatase that associates with Cdk2. Cell 75, 791–803.
Hausauer DL, Gerami-Nejad M, Kistler-Anderson C, Gale CA (2005). Hyphal guidance and invasive growth in *Candida albicans* require the Ras-like GTPase Rsr1p and its GTPase-activating protein Bud2p. Eukaryot Cell 4, 1273–1286.
Hazbun TR *et al*. (2003). Assigning function to yeast proteins by integration of technologies. Mol Cell 12, 1353–1365.
Howell AS, Lew DJ (2012). Morphogenesis and the cell cycle. Genetics 190, 51–77.
Huang CF, Liu YW, Tung L, Lin CH, Lee FJ (2003). Role for Arf3p in development of polarity, but not endocytosis, in *Saccharomyces cerevisiae*. Mol Biol Cell 14, 3834–3847.
Irazoqui JE, Lew DJ (2004). Polarity establishment in yeast. J Cell Sci 117, 2169–2171.
Jin R, Dobry CJ, McCown PJ, Kumar A (2008). Large-scale analysis of yeast filamentous growth by systematic gene disruption and overexpression. Mol Biol Cell 19, 284–296.
Kang PJ, Beven L, Hariharan S, Park HO (2010). The Rsr1/Bud1 GTPase interacts with itself and the Cdc42 GTPase during bud-site selection and polarity establishment in budding yeast. Mol Biol Cell 21, 3007–3016.
Kozminski KG, Beven L, Angerman E, Tong AH, Boone C, Park HO (2003). Interaction between a Ras and a Rho GTPase couples selection of a growth site to the development of cell polarity in yeast. Mol Biol Cell 14, 4958–4970.
Kupzig S *et al.* (2006). GAP1 family members constitute bifunctional Ras and Rap GTPase-activating proteins. J Biol Chem 281, 9891–9900.
Lambert AA, Perron MP, Lavoie E, Pallotta D (2007). The *Saccharomyces cerevisiae* Arf3 protein is involved in actin cable and cortical patch formation. FEMS Yeast Res 7, 782–795.
Leberer E, Chenevert J, Leeuw T, Harcus D, Herskowitz I, Thomas DY (1996). Genetic interactions indicate a role for Mdg1p and the SH3 domain protein Bem1p in linking the G-protein mediated yeast pheromone signalling pathway to regulators of cell polarity. Mol Gen Genet 252, 608–621.
Lo WS, Dranginis AM (1998). The cell surface flocculin Flo11 is required for pseudohyphae formation and invasion by *Saccharomyces cerevisiae*. Mol Biol Cell 9, 161–171.
Longtine MS, McKenzie A 3rd, Demarini DJ, Shah NG, Wach A, Brachat A, Philippsen P, Pringle JR (1998). Additional modules for versatile and economical PCR-based gene deletion and modification in *Saccharomyces cerevisiae*. Yeast 14, 953–961.
Osmani N, Peglion F, Chavrier P, Etienne-Manneville S (2010). Cdc42 localization and cell polarity depend on membrane traffic. J Cell Biol 191, 1261–1269.
Palecek SP, Parikh AS, Kron SJ (2002). Sensing, signalling and integrating physical processes during *Saccharomyces cerevisiae* invasive and filamentous growth. Microbiology 148, 893–907.
Pan X, Harashima T, Heitman J (2000). Signal transduction cascades regulating pseudohyphal differentiation of *Saccharomyces cerevisiae*. Curr Opin Microbiol 3, 567–572.
Park HO, Bi E (2007). Central roles of small GTPases in the development of cell polarity in yeast and beyond. Microbiol Mol Biol Rev 71, 48–96.
Park HO, Chant J, Herskowitz I (1993). BUD2 encodes a GTPase-activating protein for Bud1/Rsr1 necessary for proper bud-site selection in yeast. Nature 365, 269–274.
Park HO, Kang PJ, Rachfal AW (2002). Localization of the Rsr1/Bud1 GTPase involved in selection of a proper growth site in yeast. J Biol Chem 277, 26721–26724.
Park HO, Sanson A, Herskowitz I (1999). Localization of Bud2p, a GTPase-activating protein necessary for programming cell polarity in yeast to the presumptive bud site. Genes Dev 13, 1912–1917.
Perez P, Rincon SA (2010). Rho GTPases: regulation of cell polarity and growth in yeasts. Biochem J 426, 243–253.
Rivera-Molina FE, Novick PJ (2009). A Rab GAP cascade defines the boundary between two Rab GTPases on the secretory pathway. Proc Natl Acad Sci USA 106, 14408–14413.
Sabe H (2003). Requirement for Arf6 in cell adhesion, migration, and cancer cell invasion. J Biochem 134, 485–489.
Sikorski RS, Hieter P (1989). A system of shuttle vectors and yeast host strains designed for efficient manipulation of DNA in *Saccharomyces cerevisiae*. Genetics 122, 19–27.
Smaczynska-de R II, Costa R, Ayscough KR (2008). Yeast Arf3p modulates plasma membrane PtdIns(4,5)P2 levels to facilitate endocytosis. Traffic 9, 559–573.
Sudbery PE (2011). Growth of *Candida albicans* hyphae. Nat Rev Microbiol 9, 737–748.
Tsai PC, Lee SW, Liu YW, Chu CW, Chen KY, Ho JC, Lee FJ (2008). Afi1p functions as an Arf3p polarization-specific docking factor for development of polarity. J Biol Chem 283, 16915–16927.
Vernet T, Dignard D, Thomas DY (1987). A family of yeast expression vectors containing the phage f1 intergenic region. Gene 52, 225–233.
Wu X, Jiang YW (2005). Genetic/genomic evidence for a key role of polarized endocytosis in filamentous differentiation of *S. cerevisiae*. Yeast 22, 1143–1153.
Zakrzewska E, Perron M, Laroche A, Pallotta D (2003). A role for GEA1 and GEA2 in the organization of the actin cytoskeleton in *Saccharomyces cerevisiae*. Genetics 165, 985–995.